

# Two-Stage Robust Planning Model for Park-Level Integrated Energy System Considering Uncertain Equipment Contingency

Zuxun Xiong, Xinwei Shen\*, Hongbin Sun

**Abstract**—In this paper, we propose a two-stage robust planning model for an Integrated Energy System (IES) that serves an industrial park. The term “Park-level IES” is used to refer to IES of a smaller scale but have high demands for various forms of energy. The proposed planning model considers uncertainties like load demand fluctuations and equipment contingencies, and provides a reliable scheme of equipment selection and sizing for IES investors. Inspired by the unit commitment problem, we formulate an equipment contingency uncertainty set to accurately describe the potential equipment contingencies which happen and can be repaired within a day. Then, a novel and modified nested column-and-constraint generation algorithm is applied to solve this two-stage robust planning model with integer recourse efficiently. In the case study, the role of energy storage system for IES reliability enhancement is analyzed in detail. Computational results demonstrate the advantage of the proposed models over the deterministic planning model in terms of improving reliability.

**Index Terms**—Park-level Integrated Energy System, robust planning model, energy storage system, nested column-and-constraint generation.

## I. INTRODUCTION

WITH the rapid development of Integrated Energy Systems (IESs) in recent years [1], there is an increasing need for research into new methods that can help plan and operate such systems. The model formulation of the IES is more complicated than that of traditional power systems due to the integration of components with different types of energy carriers. Furthermore, dispatchable resources such as renewable resources, multiple energy storage systems (ESS), and electric vehicles (EV) are connected to IES, which improves its flexibility but also brings significant uncertainties. All these factors lead to unprecedented complexity in relevant decision-making and pose greater challenges to the operational economy and system reliability of IES. Research related to decision-making under uncertainty in the power system is already challenging [2], and even more so for the IES that integrates different types of energy carriers.

In this paper, we focus the planning of an IES for an industrial park, a so-called park-level IES. Developing park-level IES is considered a promising approach to enhance energy utilization efficiency [3]. However, as outlined above,

there are significant uncertainty related to the planning and operation problems of these types of IES which has not been sufficiently addressed in prior research. As a result, this study focuses on the IES planning problem, where we seek to identify optimal long-term investment decisions. In addition to economic efficiency, reliability is a main focus of this study. Our goal is to invest an IES which can be operated normally under uncertain perturbations, namely a robust IES, at the minimum cost.

To assess the reliability of the IES, relevant indices and methods should be introduced. There is a comprehensive reliability assessment framework for the traditional power system. Bilinton et al. define the reliability of power system and summarize the reliability indices to reflect different characteristics [4]. Indices like loss of load frequency (LOLF), loss of load expectation (LOLE) and expected energy not supplied (EENS) are widely used to evaluate the reliability of power systems. They can also be applied to evaluate IES reliability since they can reflect the operating status of a system regardless of the energy type. The reliability assessment techniques fall into two categories: analytical and simulation methods. Analytical methods use models to mathematically calculate reliability indices [5], while simulation approaches, e.g., Monte Carlo Simulation (MCS), estimate these indices by simulating the system's actual and random processes [6]. Both techniques are applicable for evaluating IES reliability [7].

Although the reliability assessment method has been widely studied, this process is a posteriori, i.e., the assessment result is given only after the construction plan and operation scheme of the energy system are known. To address this limitation, researchers have focused on integrating reliability indices into the planning models of the IES, leading to reliability-based planning approaches. The aim of these studies is to provide a planning scheme that will enable the IES to operate normally despite potential uncertain interference. These studies can be further divided into two categories based on the sources of uncertainty they consider.

The first group of studies primarily focuses on external uncertainty such as variations in renewable resource output and fluctuating load demands. Reference [8] proposes a two-stage RO model for energy storage planning, taking into account random wind output and uncertain load in the system. The numerical cases show that the planning results can make the system immune to the fluctuations of the considered uncertainty, and no more load shedding occurs, thus improving the system reliability. Stefano et al. propose a robust opti-

\*Xinwei Shen is with the Institute for Ocean Engineering, Tsinghua Shenzhen International Graduate School, Tsinghua University, Shenzhen 518055, China (e-mail: sxw.tbsi@sz.tsinghua.edu.cn).

This work is partly supported by Natural Science Foundation of China under No. 52007123 (Corresponding: Xinwei Shen).

mization framework for long-term energy system planning that considers various external uncertainties [9] and apply it to plan the real-world European power system [10]. The analysis verifies the effectiveness of the proposed framework in terms of improving reliability and avoiding over-investment.

While external uncertainties affect system reliability, the internal uncertainties such as the failure of critical components like transmission lines and generators, have a more immediate and substantial impact on system reliability. Consequently, the second group of reliability-based planning methods places greater emphasis on addressing challenges arising from component contingencies. A common approach is introducing security constraints. Reference [11] refers to the N-1 security criterion, which is widely used in power system planning, and then proposes a planning model for coupled electricity-gas transmission systems. Our previous study also proposes an N-1 planning model for park-level IES [12]. This criterion is extended to an N-k- $\epsilon$  criterion, and integrated into a planning model [13].

Due to the over conservatism of the N-1 criterion, some studies integrate the reliability assessment process into the planning model and use reliability metrics as constraints to ensure system stability. For example, the simulation method is combined with the planning model to calculate relevant reliability indices [14]–[18]. To be specific, [14] generates numerous scenarios to simulate microgrid operation, considering the component outages and uncertain renewable resources output to calculate and limit the LOLE. A tri-level power system expansion planning framework is proposed by [15]. Its first two levels correspond to construction and operation decisions respectively, and the third level applies MCS for reliability assessment. If the reliability index does not meet the criteria, the reliability subproblem of the third level will add the reliability dual cut back to the first level. Finally, the solution converges and provides the optimal planning scheme. A similar three-stage planning model for electricity and gas systems is proposed by [16]. An N-1 security check is executed in one of its subproblems. [17] refers to the risk measures Value-at-Risk (VaR) and Conditional Value-at-Risk (CVaR), which are widely used in financial markets, and uses them as reliability indices for power system. Using Benders Decomposition, the model divides the problem into three subproblems and calculates the reliability indices in one of them using MCS. [18] proposes a bi-level optimal ESS planning model for IES, which generates scenarios based on a two-status model for component and applies MCS method to calculate the EENS of the system. Analytical approach has also been integrated into the planning model. Reference [19] uses analytical approach to evaluate the LOLE of the planning scheme for electricity and gas system, then constructs relevant constraints and adds them back to the planning model. Based on graph theory, [20] innovatively proposes an expansion planning model which explicitly incorporates analytical reliability assessment for distribution networks.

Although these works provide some references for improving energy system reliability, there are still gaps that should be filled in this field. On the one hand, existing studies mainly focus on the reliability of large-scale systems, while

neglecting that of small-scale systems which integrate generation, transmission, distribution, and utilization. However, park-level IES has become the main consumer of different kinds of energy [21], with high demands for economic efficiency and reliability. On the other hand, existing studies mainly focus on external uncertainties and either ignore the impact of component contingencies on system reliability or do not consider these contingencies properly. For example, when considering a component contingency, most existing studies assume this component is out of operation during the whole planning period instead of a specific period [11]–[13], [16], [18], [22]. This assumption makes the model too conservative and improves the reliability of the system at a large cost.

To address these problems, this paper proposes a two-stage robust planning model for park-level IES. Both external uncertainties and equipment contingencies are taken into account by the proposed model. To accurately model the equipment contingencies, we propose an equipment contingency uncertainty set. Furthermore, we develop a dedicated solution algorithm for solving the model. Simulation is carried out in a real-world industrial park to verify the effectiveness of the proposed model and algorithm. The main contributions of this paper are:

- 1) We propose a two-stage robust planning model to make a tradeoff between economy and reliability for the park-level IES. In the first stage, we optimize the planning scheme which includes the decisions on equipment selection and sizing. Then the second stage seeks for optimal operation scheme, which includes the dispatch solutions of generators and ESS, to against the worst-case scenario that found by the uncertainty sets. The worst-case scenario here is determined by a combination of external uncertainties and equipment contingencies.
- 2) We apply a novel nested column-and-constraint generation (C&CG) algorithm to solve the planning problem efficiently and analyze the convergence performance of this algorithm. Specifically, we use Karush-Kuhn-Tucker (KKT) conditions and strong duality property to reformulate the inner layer problem respectively and make a detailed comparison between these two methods.
- 3) Based on the numerical case, we analyze the effect of different budgets of the proposed uncertainty set on the planning results in detail. The role of ESS in improving IES reliability is also analyzed.

The rest of the paper is organized as follows. Section II formulates the two-stage robust IES planning model based on the Energy Hub (EH) model. Section III introduces the solving algorithms. Section IV presents the results of the case study and analyzes them in detail. The conclusion drawn from the case study is provided in Section V.

## II. TWO-STAGE ROBUST IES PLANNING MODEL

### A. Planning Model Formulation

As we mentioned, the main object of this study is the park-level IES. Due to its relatively small scale, it is unnecessary to consider its energy transmission network. We use the EH model, which reflects the relationship between energy input and output [23], for IES modeling. We follow the planning

model of our previous study [12], where three forms of energy are considered, i.e. electricity, heat, and cooling. The model makes decisions regarding the installation of combined cooling, heat and power (CCHP) units, gas boilers (GB), and electric chillers (EC), and can also choose to import power from a substation (SUB). We also introduce multi-energy ESS, e.g., battery ESS (BESS) and thermal ESS (TESS), as an option in this model. We will use B and T as abbreviation for BESS and TESS later. Based on the EH hub and the proposed equipment contingency set, we formulate the two-stage robust planning model for IES as follows.

1) *Objective Function*: The objective function minimizes the total cost. To reflect the impact of uncertainties and ensure robustness, we formulate it in the following two-stage structure:

$$\min_{X \in \mathbb{X}} f^{\text{inv}} + \max_{l \in \mathbb{L}, s \in \mathbb{S}} \min_{(Z, P) \in F(x, l, s)} f_0^{\text{ope}} + f_1^{\text{shed}}, \quad (1a)$$

$$f^{\text{inv}} = \sum_{\text{Equi}} \sum_{n \in \{i, j, k\}} IC_n^{\text{Equi}} X_n^{\text{Equi}} + \sum_{\text{ESS}} IC^{\text{ESS}} X^{\text{ESS}}, \quad (1b)$$

$$f_0^{\text{ope}} = m \sum_t [P_{0,t}^{\text{SUB}} r_t^e + (\sum_i P_{0,i,t}^{\text{CCHP}} + \sum_j P_{0,j,t}^{\text{GB}}) r_t^g], \quad (1c)$$

$$f_1^{\text{shed}} = m \sum_t \sum_{d \in \{e, h, c\}} P_{1,t}^{\text{LS},d} p_t^{\text{LS},d}, \quad (1d)$$

$$\text{Equi} \in \{\text{CCHP}, \text{GB}, \text{EC}\}, \quad \text{ESS} \in \{\text{B}, \text{T}\}.$$

Here, the objective function (1a) minimizes the total investment cost, defined by the function  $f^{\text{inv}}$ , as well as the worst-case operational cost across all possible load and equipment failure scenarios, denoted by  $\mathbb{L}$  and  $\mathbb{S}$ . This worst-case cost is defined by the max-min function which considers both the operational cost and load shed penalty, defined by the functions  $f_0^{\text{ope}}$  and  $f_1^{\text{shed}}$ , respectively. The sets  $\mathbb{L}$  and  $\mathbb{S}$  are the uncertainty sets for loads and equipment operating status. Continuous variables  $P$  and binary variables  $Z$  are second-stage operational decisions which represent the output of equipment and the storage status of ESS ( $Z = 1$  for charging and  $Z = 0$  for discharging) respectively. The feasible set of the second stage, represented by  $F(\bullet)$ , is a function of  $X$ ,  $l$ , and  $s$ . Note that the second-stage variables  $P$  and  $Z$  are fully adaptive to any realization of the uncertainties [24].

Equation (1b) shows that the investment cost includes the investment of all kinds of optional equipment and ESS. Here  $\text{Equi} \in \{\text{CCHP}, \text{GB}, \text{EC}\}$ ,  $n$  could be  $i, j, k$  when  $\text{Equi}$  stands for different type of equipment. The binary variable  $X_n^{\text{Equi}}$  is the first-stage investment decision variable which decides the construction scheme of the  $n^{\text{th}}$  equipment ( $X = 1$  if the equipment is being built and  $X = 0$  if not), and give rise to the expression for the investment cost in (1b).  $X^{\text{ESS}}$  with  $\text{ESS} \in \{\text{B}, \text{T}\}$  is a continuous decision variable, representing the capacity of ESS to be built. The investment cost is represented by the parameters  $IC_n^{\text{Equi}}$  for 3 types of equipment and  $IC^{\text{ESS}}$  for ESS.

Equation (1c) is the operational cost, which reflects the cost of procuring electricity and natural gas. We use subscripts 0 and 1 to denote normal operation scenario and scenario with contingencies, respectively.  $P_{0,n,t}^{\text{Equi}}$  represents the power output of equipment  $n$  at time  $t$  in normal operation scenario.  $r_t^e$  and

$r_t^g$  stand for time-of-use price of electricity and natural gas respectively. In (1d),  $P_{1,t}^{\text{LS},d}$  with  $d \in \{e, h, c\}$  represents the electricity, heating or cooling loads shedding, respectively, and  $p^{\text{LS},d}$  is the corresponding penalty cost coefficient for each type of load. We use  $m$  to convert all the operational costs in the planning period into the planning year through the discount rate  $\gamma$ :

$$m = \sum_{y=1}^{PP} \frac{365}{(1+\gamma)^{y-1}}, \quad (2)$$

where  $PP$  represents the total years of the planning period.

2) *Constraints*: As we mentioned, we divide variables into two sets. For normal operation scenario, the constraints can be expressed as:

$$\mathbf{L} \leq \mathbf{C}^{\text{SUB}} \mathbf{P}_0^{\text{SUB}} + \sum_{\text{Equi}} \mathbf{C}^{\text{Equi}} \mathbf{P}_0^{\text{Equi}} - \mathbf{P}_0^{\text{ESS}}, \quad (3a)$$

$$l_t^e \leq C_{e-e}^{\text{SUB}} P_{0,t}^{\text{SUB}} + \sum_i C_{i,g-e}^{\text{CCHP}} P_{0,i,t}^{\text{CCHP}} + \sum_k C_{k,e-e}^{\text{EC}} P_{0,k,t}^{\text{EC}} - P_{0,dis,t}^{\text{B}} + P_{0,dis,t}^{\text{T}}, \quad (3b)$$

$$l_t^h \leq \sum_i C_{i,g-h}^{\text{CCHP}} P_{0,i,t}^{\text{CCHP}} + \sum_j C_{j,g-h}^{\text{GB}} P_{0,j,t}^{\text{GB}} - P_{0,dis,t}^{\text{T}} + P_{0,dis,t}^{\text{B}}, \quad (3c)$$

$$l_t^c \leq \sum_i C_{i,g-c}^{\text{CCHP}} P_{0,i,t}^{\text{CCHP}} + \sum_k C_{k,e-c}^{\text{EC}} P_{0,k,t}^{\text{EC}}, \quad (3d)$$

$$P_{n,min}^{\text{Equi}} X_n^{\text{Equi}} \leq P_{0,n,t}^{\text{Equi}} \leq P_{n,max}^{\text{Equi}} X_n^{\text{Equi}}, \quad (3e)$$

$$\sum_t P_{0,ch,t}^{\text{B}} - T_{max}^{\text{ch}} X^{\text{B}} \leq 0, \quad (3f)$$

$$\text{SoC}_{min}^{\text{B/T}} X^{\text{B/T}} \leq E_{0,t}^{\text{B/T}} \leq \text{SoC}_{max}^{\text{B/T}} X^{\text{B/T}}, \quad (3g)$$

$$0 \leq P_{0,ch,t}^{\text{B/T}} \leq M Z_{0,ch,t}^{\text{B/T}}, \quad (3h)$$

$$0 \leq P_{0,dis,t}^{\text{B/T}} \leq M(1 - Z_{0,dis,t}^{\text{B/T}}), \quad (3i)$$

$$P_{0,ch/dis,t}^{\text{B/T}} \leq \text{coe}_{ch/dis}^{\text{B/T}} X^{\text{B/T}}, \quad (3j)$$

$$E_{0,t}^{\text{B/T}} = E_{0,t-1}^{\text{B/T}} + P_{0,ch,t-1}^{\text{B/T}} \eta_{ch}^{\text{B/T}} - P_{0,dis,t-1}^{\text{B/T}} / \eta_{dis}^{\text{B/T}}, \quad (3k)$$

$$0 \leq P_{0,t}^{\text{SUB}} \quad (3l)$$

$$X \in \mathbb{X} = \{X^{\text{ESS}} \geq 0, X_n^{\text{Equi}} \in \{0, 1\}\}, \quad (3m)$$

$$Z_{ch,t}^{\text{B/T}} \in \{0, 1\}, l \in \mathbb{L}, s \in \mathbb{S}, \quad (3n)$$

$$\forall 1 \leq t \leq \text{Period},$$

$$\forall 1 \leq i \leq N^{\text{CCHP}}, \quad \forall 1 \leq j \leq N^{\text{GB}}, \quad \forall 1 \leq k \leq N^{\text{EC}}.$$

Here  $\text{Period}$  is the length of the planning period,  $N^{\text{Equi}}$  represents the number of optional equipment of a certain type. Equation (3a) is the supply-demand balance constraint under normal operation scenario formulated based on EH model. where  $\mathbf{L}$  denotes the loads of IES.  $\mathbf{P}^{\text{Equi}}$  denotes the output of different equipment,  $\mathbf{C}^{\text{Equi}}$  represents the coupling matrix of different equipment and the subscripts indicate different kinds of energy. For example,  $C_{i,g-e}^{\text{CCHP}}$  represents the efficiency of the  $i^{\text{th}}$  CCHP in converting natural gas into electricity. All supply must be equal or larger than the demand at any time under normal operation scenario (no shedding load is allowed).  $\mathbf{P}^{\text{ESS}}$  denotes the matrix of charge/discharge power of BESS and TESS. The subscript  $ch$  and  $dis$  denote charge and discharge, respectively. Constraint (3a) can be further expressed

as (3b)—(3d). As indicated by constraint (3e), the output of each equipment is bounded by both its lower/upper limit and its investment state  $X_n^{\text{Equi}}$ .  $T_{max}^{\text{ch}}$  represents the maximum charging cycle of the BESS. Constraint (3f) limits the maximum charge amount. Constraint (3g) limits the state of charge (SoC) level of ESS between a certain range, where  $E_t^{\text{ESS}}$  represents the stored energy of ESS at time  $t$ . Constraints (3h) and (3i) guarantee that there will be no simultaneous charging and discharging by using a large constant  $M$ . Constraint (3j) limits the charge and discharge rate of ESS. Equation (3k) represents the energy variation of the ESS during the whole period. Constraint (3l) means we can get electricity from the substation outside the IES. We denote constraints for ESS under normal operation scenario, i.e., (3f)—(3k), as:

$$\text{Cons}_0^{\text{ESS}}(X^{\text{B/T}}, P_{0,\text{ch/dis},t}^{\text{B/T}}, Z_{0,\text{ch},t}^{\text{B/T}}, E_{0,t}^{\text{B/T}}). \quad (4)$$

For constraints under scenario with contingencies, we add load shedding term to the supply-demand balance constraint to guarantee the feasibility of the problem:

$$\mathbf{L} \leq \mathbf{C}^{\text{SUB}} \mathbf{P}_1^{\text{SUB}} + \mathbf{C} \mathbf{P}_1^{\text{Equi}} - \mathbf{P}_1^{\text{ESS}} + \mathbf{P}_1^{\text{LS}}. \quad (5)$$

Constraints on shedding load  $P_{1,t}^{\text{LS},d} \geq 0$  should also be considered. Then, the upper and lower limits of equipment output are constrained by both the investment decision variable  $X$  and the operation state variable  $s$ :

$$P_{n,\min}^{\text{Equi}} s_{n,t}^{\text{Equi}} X_n^{\text{Equi}} \leq P_{1,n,t}^{\text{Equi}} \leq P_{n,\max}^{\text{Equi}} s_{n,t}^{\text{Equi}} X_n^{\text{Equi}} \quad (6)$$

which is different from that of the normal operation scenario as shown in constraint (3e). Constraint (6) indicates that even if the equipment is invested, its output power will be 0 when it fails ( $s = 0$ ). The ESS-related constraints under scenario with contingency are almost the same as those under normal operation scenario, we denote these ESS-related constraints as follow for convenience:

$$\text{Cons}_1^{\text{ESS}}(X^{\text{B/T}}, P_{1,\text{ch/dis},t}^{\text{B/T}}, Z_{1,\text{ch},t}^{\text{B/T}}, E_{1,t}^{\text{B/T}}). \quad (7)$$

Besides, the constraint for substation will be  $P_{1,t}^{\text{SUB}} \geq 0$ .

### B. Uncertainty Set Formulation

In this part, we propose a unique uncertainty set to describe equipment contingencies inspired by typical Unit Commitment (UC) problem [24]. UC problem involves determining which and when generating units should be turned on and turned off over a certain period of time, typically ranging from several hours to a few days. There are resemblances between the modeling of unit on/off states in UC problem and the operating statuses of equipment in our problem. For example, the constraints associated with turn-on and turn-off actions of the UC problem can be used to describe the start point and end point of an equipment contingency. The minimum up and minimum down times constraints of the UC problem can be used to describe the duration of an equipment contingency.

With this insight, we formulate the following uncertainty set for equipment contingencies:

$$\mathbb{S} = \left\{ \begin{array}{l} \sum_{\text{Equi}} \sum_n s_{n,t}^{\text{Equi}} \geq \sum_{\text{Equi}} N^{\text{Equi}} - \Gamma^N \\ \sum_{\text{Equi}} \sum_{v=t-\Gamma_n^I+1}^t y_{n,v}^{\text{Equi}} \leq 1, \quad t \in [\Gamma_n^I, \text{Period}] \\ \sum_{v=t-\Gamma_n^D+1}^t y_{n,v}^{\text{Equi}} = 1 - s_{n,t}^{\text{Equi}}, \quad t \in [\Gamma_n^D, \text{Period}] \\ s_{n,t}^{\text{Equi}} \in \{0, 1\}, y_{n,t}^{\text{Equi}} \in \{0, 1\} \end{array} \right\},$$

where  $s_{n,t}^{\text{Equi}}$  represent the operation state of equipment  $n$  at time  $t$ .  $y_{n,v}^{\text{Equi}}$  is a binary variable indicating the starting point of a certain contingency of the equipment  $n$ . All  $\Gamma$  are the constants used to control the conservativeness of the model, which we also call budgets. For example,  $\Gamma^N$  is a budget for the number of simultaneously failed equipment. When it equals to 2, the first constraint of the uncertain set  $\mathbb{S}$  means that up to 2 equipment are out of operation at the time  $t$ . The second and third constraints are used to describe the interval between two sequential contingencies and the duration of each equipment contingency.

As for the multi-energy loads, we formulate its uncertainty set as:

$$\mathbb{L} = \left\{ \begin{array}{l} \bar{l}_t^d + \Delta l_t^d \leq l_t^d \leq \bar{l}_t^d - \Delta l_t^d \\ \sum_{t=1}^{\text{Period}} \frac{|l_t^d - \bar{l}_t^d|}{\Delta l_t^d} \leq \Gamma^l, d \in \{e, h, c\} \end{array} \right\}$$

### III. SOLVING METHOD

In this section, we will first give a brief introduction to the C&CG algorithm and nested C&CG algorithm. Then, the proposed two-stage robust planning model will be reformulated into a structure that can be well solved by nested C&CG. After that, the whole solving process of the proposed planning model and relevant algorithms will be presented in detail.

#### A. Preliminary

We first take the following typical two-stage robust model as an example:

$$\begin{aligned} \min_y \mathbf{c}^T \mathbf{y} + \max_{\mathbf{u} \in \mathbb{U}} \min_{\mathbf{x} \in F(\mathbf{y}, \mathbf{u})} \mathbf{b}^T \mathbf{x} \\ \mathbf{y} \in \mathbf{S}_y : \mathbf{A} \mathbf{y} \geq \mathbf{d} \\ \mathbf{x} \in \mathbf{S}_x : \mathbf{G} \mathbf{x} \geq \mathbf{h} - \mathbf{E} \mathbf{y} - \mathbf{M} \mathbf{u} \end{aligned} \quad (\text{P1})$$

Here  $\mathbf{y}$  is the first-stage variable,  $\mathbb{U}$  is the uncertainty set and  $\mathbf{x}$  is the second-stage variable, which is continuous. According to the previous studies, even a simple two-stage RO model as shown in (P1) is a hard-to-solve NP-hard problem unless  $\mathbb{U}$  only has finite elements. With finite elements in  $\mathbb{U}$ , (P1) can be reformulated into an easy-to-solve problem as follow:

$$\begin{aligned} \min_y \mathbf{c}^T \mathbf{y} + \eta \\ \mathbf{y} \in \mathbf{S}_y, \quad \mathbf{A} \mathbf{y} \geq \mathbf{d} \\ \mathbf{x}^l \in \mathbf{S}_x, \quad \eta \geq \mathbf{b}^T \mathbf{x}^l, \mathbf{E} \mathbf{y} + \mathbf{G} \mathbf{x}^l \geq \mathbf{h} - \mathbf{M} \mathbf{u}_l, l = 1, \dots, r \end{aligned} \quad (\text{P2})$$

Obviously, even a two-stage robust model with an infinite uncertainty set can be solved easily if we can find finite nontrivial elements from its uncertainty set. This is the basic idea of the C&CG algorithm [25]. To do so, it splits the original problem (P1) into a master problem (MP<sub>1</sub>) and a subproblem (SP<sub>1</sub>), which can be shown as follows, then solves them respectively and finds the nontrivial values of  $\mathbb{U}$  from the subproblem through iteration.

$$\begin{aligned} & \min_{\mathbf{y}, \eta} \mathbf{c}^T \mathbf{y} + \eta \\ & \eta \in \mathbb{R}, \quad \eta \geq \mathbf{b}^T \mathbf{x}^l, \quad \forall l \in \mathbf{O} \\ & \mathbf{x}^l \in \mathbf{S}_{\mathbf{x}}, \quad \mathbf{E}\mathbf{y} + \mathbf{G}\mathbf{x}^l \geq \mathbf{h} - \mathbf{M}\mathbf{u}_l^*, \quad \forall l \leq k \end{aligned} \quad (\text{MP}_1)$$

Here  $\mathbf{O}$  starts from an empty set.  $k$  indicates the number of the iterations and starts with 0.  $\mathbf{u}_l^*$  is the solution obtained from (SP<sub>1</sub>).

$$\mathcal{Q}(\hat{\mathbf{y}}) = \left\{ \max_{\mathbf{u} \in \mathbb{U}} \min_{\mathbf{x}} \mathbf{b}^T \mathbf{x} : \mathbf{G}\mathbf{x} \geq \mathbf{h} - \mathbf{E}\hat{\mathbf{y}} - \mathbf{M}\mathbf{u}, \mathbf{x} \in \mathbf{S}_{\mathbf{x}} \right\} \quad (\text{SP}_1)$$

We first solve the MP<sub>1</sub>, obtain optimal  $\mathbf{y}_{k+1}^*$  and  $\eta_{k+1}^*$ . The solution of (MP<sub>1</sub>) provides a lower bound of the original problem. Then we solve the (SP<sub>1</sub>) to obtain a nontrivial value  $\mathbf{u}_l^*$  of uncertainty set and update the upper bound as  $\min \{UB, \mathbf{c}^T \mathbf{y}_{k+1}^* + \mathcal{Q}(\mathbf{y}_{k+1}^*)\}$ . The subproblem is a max-min problem, which can be reformulated by KKT conditions or strong duality theory and solved easily. If the upper bound and lower bound converge, terminate the iteration. Otherwise, create variables  $\mathbf{x}^{k+1}$  and add constraints  $\eta \geq \mathbf{b}^T \mathbf{x}^{k+1}$  and  $\mathbf{E}\mathbf{y} + \mathbf{G}\mathbf{x}^{k+1} \geq \mathbf{h} - \mathbf{M}\mathbf{u}_{k+1}^*$  back to the (MP<sub>1</sub>), then update  $k = k + 1$ ,  $\mathbf{O} = \mathbf{O} \cup \{k + 1\}$  and begin the next iteration. It can be proved that the master problem and the subproblem will converge to the optimal result in a finite number of iterations.

In the solution process of the C&CG, the subproblem is solved by using KKT conditions or strong duality theory. However, the prerequisite for using both methods to solve the subproblem is that the problem satisfies the strong duality. Two-stage RO model with integer recourse (the second-stage variable), e.g., the proposed IES planning problem, cannot be solved by C&CG directly as its subproblem does not meet the prerequisite. For example, if there are integer variables in the second stage of (P1), the subproblem SP<sub>1</sub> should be written as:

$$\mathcal{Q}(\hat{\mathbf{y}}) = \left\{ \begin{array}{l} \max_{\mathbf{u} \in \mathbb{U}} \min_{\mathbf{x}_1, \mathbf{x}_2} \mathbf{b}_1^T \mathbf{x}_1 + \mathbf{b}_2^T \mathbf{x}_2 : \\ \mathbf{G}_1 \mathbf{x}_1 + \mathbf{G}_2 \mathbf{x}_2 \geq \mathbf{h} - \mathbf{E}\hat{\mathbf{y}} - \mathbf{M}\mathbf{u} \\ \mathbf{x}_1 \in \mathbb{Z}_+^n, \quad \mathbf{x}_2 \in \mathbb{R}_+^p \end{array} \right\}. \quad (\text{SP}_2)$$

Here we divide  $\mathbf{x}$  into a vector of integer variables  $\mathbf{x}_1$  and a vector of continuous variables  $\mathbf{x}_2$ . Obviously, KKT conditions cannot be directly used to transform this max-min problem into a min problem due to the existence of integer  $\mathbf{x}_1$ . To solve this max-min subproblem, we should first formulate its objective function into an equivalent tri-level form by separating terms related to  $\mathbf{x}_1$  and those related to  $\mathbf{x}_2$ :

$$\mathcal{Q}(\hat{\mathbf{y}}) = \max_{\mathbf{u} \in \mathbb{U}} \min_{\mathbf{x}_1 \in \Phi} \mathbf{b}_1^T \mathbf{x}_1 + \min_{\mathbf{x}_2} \mathbf{b}_2^T \mathbf{x}_2. \quad (8)$$

The subproblem now can be solved by using the countability of  $\Phi$ . C&CG algorithm can also be used to solve this subproblem faster by finding the nontrivial value of  $\Phi$  efficiently.

In summary, we can solve a two-stage robust model with integer recourse by using an outer layer C&CG algorithm on the basis of solve its subproblem with an inner layer C&CG. This is the nested C&CG algorithm [26].

### B. Two-Stage Robust Planning Model Reformulation

The proposed two-stage robust planning model can be reformulated into a master problem and a subproblem. Naturally, the master problem will be:

$$\text{MP: } \min_{X \in \mathbb{X}} \sum_{\text{Equi}} \sum_n IC_n^{\text{Equi}} X_n^{\text{Equi}} + \sum_{\text{ESS}} IC^{\text{ESS}} X^{\text{ESS}} + \psi, \quad (9a)$$

$$\begin{aligned} s.t. \quad & \psi \geq m \sum_t [P_{0,t,q}^{\text{SUB}} r_t^e + (\sum_i P_{0,i,t,q}^{\text{CCHP}} + \sum_j P_{0,j,t,q}^{\text{GB}}) r_t^g + \\ & P_{1,t,q}^{\text{LS},d} p_t^{\text{LS},d}], \end{aligned} \quad (9b)$$

$$\tilde{\mathbf{L}} \leq \mathbf{C}^{\text{SUB}} \mathbf{P}_{0,q}^{\text{SUB}} + \mathbf{C} \mathbf{P}_{0,q}^{\text{Equi}} - \mathbf{P}_{0,q}^{\text{ESS}}, \quad (9c)$$

$$\tilde{\mathbf{L}} \leq \mathbf{C}^{\text{SUB}} \mathbf{P}_{1,q}^{\text{SUB}} + \mathbf{C} \mathbf{P}_{1,q}^{\text{Equi}} - \mathbf{P}_{1,q}^{\text{ESS}} + \mathbf{P}_{1,q}^{\text{LS}}, \quad (9d)$$

$$P_{n,\min}^{\text{Equi}} X_n^{\text{Equi}} \leq P_{0,n,t,q}^{\text{Equi}} \leq P_{n,\max}^{\text{Equi}} X_n^{\text{Equi}}, \quad (9e)$$

$$P_{n,\min}^{\text{Equi}} \tilde{s}_{n,t}^{\text{Equi}} X_n^{\text{Equi}} \leq P_{1,n,t,q}^{\text{Equi}} \leq P_{n,\max}^{\text{Equi}} \tilde{s}_{n,t}^{\text{Equi}} X_n^{\text{Equi}}, \quad (9f)$$

$$\text{Cons}_{0,q}^{\text{ESS}}(X^{\text{B/T}}, P_{0, \text{ch}/\text{dis}, t, q}^{\text{B/T}}, Z_{0, \text{ch}, t, q}^{\text{B/T}}, E_{0, t, q}^{\text{B/T}}), \quad (9g)$$

$$\text{Cons}_{1,q}^{\text{ESS}}(X^{\text{B/T}}, P_{1, \text{ch}/\text{dis}, t, q}^{\text{B/T}}, Z_{1, \text{ch}, t, q}^{\text{B/T}}, E_{1, t, q}^{\text{B/T}}), \quad (9h)$$

$$0 \leq P_{0/1, t, q}^{\text{SUB}}, \quad (9i)$$

$$0 \leq P_{1, t, q}^{\text{LS},d}, \quad (9j)$$

$$X \in \mathbb{X}, Z_{0/1, \text{ch}, t, q}^{\text{B/T}} \in \{0, 1\}, \quad (9k)$$

$$\forall 1 \leq q \leq p.$$

The nature of the decomposition solving algorithm is to solve the master problem and subproblem iteratively until they converge. Here we use subscript  $q$  to indicate the number of iterations. After each iteration, a new set of variables and constraints, which are also called *cuts*, that are generated from the subproblem will be added back to the master problem.  $\tilde{\mathbf{L}}$  represents the matrix of  $\tilde{l}_t^d$ . It should be noticed that both  $\tilde{l}_t^d$  and  $\tilde{s}^{\text{Equi}}$  are constants instead of variables in the master problem, their value can be obtained from the solution of the subproblem. The subproblem can be shown as follows:

$$\text{SP: } \mathcal{Q}(\hat{X}) = \max_{l \in \mathbb{L}, s \in \mathbb{S}} \min_{(Z, P) \in F(x, l, s)} f_0^{\text{ope}} + f_1^{\text{shed}} \quad (10)$$

$$s.t. \quad (3b) - (3k), (5) - (7), Z_{0/1, \text{ch}, t}^{\text{B/T}} \in \{0, 1\}, l \in \mathbb{L}, s \in \mathbb{S}$$

where  $\hat{X}$  is the current optimal planning decision from the master problem. The inner layer algorithm which will be introduced later can be used to solve this subproblem of max-min form.

### C. Outer Layer Algorithm

On the basis that the subproblem can be solved by the inner layer algorithm, the outer layer algorithm can be applied to solve the proposed planning model in the following steps:

- 1) *Step 1:* Set  $LB = -\infty$ ,  $UB = +\infty$  and  $p = 0$ .

2) *Step 2*: Solve the master problem **MP**.

Derive an optimal solution  $(X^*, \psi^*)$  and update  $LB = \sum_{\text{Equi}} \sum_n IC_n^{\text{Equi}} X_n^{\text{Equi},*} + \sum_{\text{ESS}} IC^{\text{ESS}} X^{\text{ESS},*} + \psi^*$ . If  $UB - LB \leq \epsilon$ , return the solution and terminate.

3) *Step 3*: Obtain  $\hat{X}$  from step 2 and solve the subproblem **SP** by inner layer algorithm. Derive an optimal solution  $(l^*, s^*)$  and update  $UB = \min\{UB, \sum_{\text{Equi}} \sum_n IC_n^{\text{Equi}} X_n^{\text{Equi},*} + \sum_{\text{ESS}} IC^{\text{ESS}} X^{\text{ESS},*} + Q^*(\hat{X})\}$ . If  $UB - LB \leq \epsilon$ , return and terminate. The details of the solution process for the subproblem can be found in inner level algorithm.

4) *Step 4*: Obtain  $(\tilde{l}, \tilde{s})$  from subproblem, update  $p = p + 1$ . Create variables  $(P_{0/1}^{q+1}, Z_{0/1}^{q+1})$  and add constraints (9b)–(9k) with index  $q = q + 1$  to the **MP**, go to *Step 2*.

The pseudocode of outer layer algorithm can be found in Algorithm 1.

---

#### Algorithm 1 Outer layer C&CG

---

**Input:**  $LB = -\inf, UB = +\inf, \epsilon = 0.0001, p = 0$

**Output:**  $X^*, Z^*, P^*$

- 1: **while**  $UB - LB \leq \epsilon$  **do**
  - 2:   Solve the MP with  $(\tilde{l}, \tilde{s})$
  - 3:   Update  $LB \rightarrow \sum_{\text{Equi}} \sum_n IC_n^{\text{Equi}} X_n^{\text{Equi},*} + \sum_{\text{ESS}} IC^{\text{ESS}} X^{\text{ESS},*} + \psi^*$
  - 4:   Solve the **SP** with  $\hat{X}$  by Algorithm 2
  - 5:   Update  $UB \rightarrow \min\{UB, \sum_{\text{Equi}} \sum_n IC_n^{\text{Equi}} X_n^{\text{Equi},*} + \sum_{\text{ESS}} IC^{\text{ESS}} X^{\text{ESS},*} + Q^*(\hat{X})\}$
  - 6:   Create variables  $(P_{0/1}^{q+1}, Z_{0/1}^{q+1})$  and add (9b)–(9k) back to **MP**
  - 7:   Update  $p \rightarrow p + 1$
  - 8: **end while**
- 

#### D. Inner Layer Algorithm

As shown in *Step 3* of the outer layer algorithm, the **SP** is solved by the inner layer algorithm. To better illustrate the inner layer algorithm, we reformulate the subproblem and get its tri-level equivalent form as follows:

$$Q(\hat{X}) = \max_{l \in \mathbb{L}, s \in \mathbb{S}} \min_{Z \in \Phi_Z} \min_P f_0^{\text{ope}} + f_1^{\text{shed}} \quad (11)$$

where  $\Phi_Z = \{Z^r\}_{r=1}^R$ . By making use of the countability of  $\Phi_Z$ , we have

$$Q(\hat{X}) = \max \sigma, \quad (12)$$

$$\text{s.t. } \sigma \leq \min\{m \sum_t [P_{0,t,r}^{\text{SUB}} r_t^e + (\sum_i P_{0,i,t,r}^{\text{CCHP}} + \sum_j P_{0,j,t,r}^{\text{GB}}) r_t^g + P_{1,t,r}^{\text{LS},d} p_t^{\text{LS},d}] : \text{Cons}_r^{\text{SP}}, r = 1, \dots, R\}. \quad (13)$$

Since there are no integer variables, the minimization problem on the right side of (13) can be converted into a feasible problem by KKT conditions directly. We can also reformulate the innermost min problem of (11) into a max problem by strong duality theory and then use another C&CG algorithm to solve the obtained max-min-max problem. This subproblem will also be reformulated into a master problem and a subproblem and solved by a decomposition algorithm. Here  $r$  is used to denote the number of inner algorithm iterations. The constraints  $\text{Cons}_r^{\text{SP}}$  are almost the same as the

constraints of the original optimization problem except with  $\hat{X}$  as constant. The inner layer algorithm follows steps as:

- 1) *Step 1*: Set  $LB_s = -\infty, UB_s = +\infty$  and  $p_s = 0$ .
- 2) *Step 2*: Solve the master problem of subproblem:

$$\text{MPs: } \max \sigma, \quad (14a)$$

$$\text{s.t. } \sigma \leq m \sum_t [P_{0,t,r}^{\text{SUB}} r_t^e + (\sum_i P_{0,i,t,r}^{\text{CCHP}} + \sum_j P_{0,j,t,r}^{\text{GB}}) r_t^g + P_{1,t,r}^{\text{LS},d} p_t^{\text{LS},d}], \quad (14b)$$

$$\mathbf{L} \leq \mathbf{C}^{\text{SUB}} \mathbf{P}_{0,r}^{\text{SUB}} + \mathbf{C} \mathbf{P}_{0,r}^{\text{Equi}} - \mathbf{P}_{0,r}^{\text{ESS}} \quad (14c)$$

$$\mathbf{L} \leq \mathbf{C}^{\text{SUB}} \mathbf{P}_{1,r}^{\text{SUB}} + \mathbf{C} \mathbf{P}_{1,r}^{\text{Equi}} - \mathbf{P}_{1,r}^{\text{ESS}} + \mathbf{P}_{1,r}^{\text{LS}} \quad (14d)$$

$$P_{n,\min}^{\text{Equi}} \hat{X}_n^{\text{Equi}} \leq P_{0,n,t,r}^{\text{Equi}} \leq P_{n,\max}^{\text{Equi}} \hat{X}_n^{\text{Equi}}, \quad (14e)$$

$$P_{n,\min}^{\text{Equi}} s_{n,t} \hat{X}_n^{\text{Equi}} \leq P_{1,n,t,r}^{\text{Equi}} \leq P_{n,\max}^{\text{Equi}} s_{n,t} \hat{X}_n^{\text{Equi}}, \quad (14f)$$

$$\text{Cons}_{0,r}^{\text{ESS}}(\hat{X}^{\text{B/T}}, P_{0,\text{ch}/\text{dis},t,r}^{\text{B/T}}, \tilde{Z}_{0,\text{ch},t,r}^{\text{B/T}}, E_{0,t,r}^{\text{B/T}}), \quad (14g)$$

$$\text{Cons}_{1,r}^{\text{ESS}}(\hat{X}^{\text{B/T}}, P_{1,\text{ch}/\text{dis},t,r}^{\text{B/T}}, \tilde{Z}_{1,\text{ch},t,r}^{\text{B/T}}, E_{1,t,r}^{\text{B/T}}), \quad (14h)$$

$$0 \leq P_{0/1,t,r}^{\text{SUB}} \quad (14i)$$

$$0 \leq P_{1,t,r}^{\text{LS},d} \quad (14j)$$

$$\text{All dual variables} \geq 0, \quad (14k)$$

$$\text{Cons}^{\text{La}}, \text{Cons}^{\text{S}}, \quad (14l)$$

$$l \in \mathbb{L}, s \in \mathbb{S}, \quad (14m)$$

$$\forall 1 \leq r \leq p_s.$$

The inner layer algorithm is also iterative, new variables and constraints with subscript  $r$  are added to the **MPs** with each iteration. Constraints (14c)–(14j) are in similar form as previous problems. However, it should be noticed that  $\hat{X}$  and  $\tilde{Z}$  are constants rather than variables in **MPs**. The former one comes from the solution of **MP**, and the latter one comes from the solution of subproblem of **SP**. Constraint (14k) is for dual variables corresponding to constraints in primal problem. In addition to the constraints of the primal problem and the constraints for dual variables, KKT conditions also contain other two groups of constraints, namely constraints for the gradient of Lagrange and the complementary slackness conditions. Here we use  $\text{Cons}^{\text{La}}$  and  $\text{Cons}^{\text{S}}$  to denote these two groups of constraints respectively as shown in (14l).

We would like to illustrate how to derive  $\text{Cons}^{\text{La}}$  and  $\text{Cons}^{\text{S}}$  instead of listing all of these constraints here. First of all,  $(P_{0/1,t,r}^{\text{SUB}}, P_{0/1,t,r}^{\text{CCHP}}, P_{0/1,t,r}^{\text{EC}}, E_{0/1,t,r}^{\text{B/T}}, P_{0/1,\text{ch}/\text{dis},t,r}^{\text{B/T}}, P_{1,t,r}^{\text{LS},d})$  is set as a group of variables of the primal problem. Then we can derive constraints by making the gradient of Lagrange with respect to each variable equal to 0. Take  $P_{0,t,r}^{\text{SUB}}$  as an example, we get:

$$mr_t^e - C_{e-e}^{\text{SUB}} \alpha_{0,t,r} - \rho_{0,t,r} = 0, \quad (15)$$

where  $\alpha_{0,t,r}$  and  $\rho_{0,t,r}$  are dual variables for constraints  $l_t^e \leq C_{e-e}^{\text{SUB}} P_{0,t,r}^{\text{SUB}} + \sum_i C_{i,g-e}^{\text{CCHP}} P_{0,i,t,r}^{\text{CCHP}} + \sum_k C_{k,e-e}^{\text{EC}} P_{0,k,t,r}^{\text{EC}} - P_{0,\text{ch},t,r}^{\text{B}} + P_{0,\text{dis},t,r}^{\text{B}}$  and  $P_{0,t,r}^{\text{SUB}} \geq 0$  respectively. We have:  $\alpha_{0,t,r}, \rho_{0,t,r} \geq 0$ . It is obvious that we can eliminate  $\rho_{0,t,r}$  and transform constraint (15) into:

$$mr_t^e - C_{e-e}^{\text{SUB}} \alpha_{0,t,r} \geq 0. \quad (16)$$

In this way we get all constraints of  $Cons^{La}$ . As for complementary slackness condition, the first constraint can be list as:

$$(-l_t^e + C_{e-e}^{SUB} P_{0,t,r}^{SUB} + \sum_i C_{i,g-e}^{CCHP} P_{0,i,t,r}^{CCHP} + \sum_k C_{k,e-e}^{EC} P_{0,k,t,r}^{EC} - P_{0,ch,t,r}^B + P_{0,dis,t,r}^B) \alpha_{0,t,r} = 0. \quad (17)$$

This is a non-linear constraint which can be reformulated to a linear constraint by using big-M method and introducing binary variables  $\nu_{t,r}$ :

$$-l_t^e + C_{e-e}^{SUB} P_{0,t,r}^{SUB} + C_{i,g-e}^{CCHP} P_{0,i,t,r}^{CCHP} + C_{k,e-e}^{EC} P_{0,k,t,r}^{EC} - P_{0,ch,t,r}^B + P_{0,dis,t,r}^B \leq M \nu_{t,r}, \quad (18)$$

$$\alpha_{0,t,r} \leq M(1 - \nu_{t,r}), \quad (19)$$

$$\nu_{t,r} \in \{0, 1\}.$$

$M$  is a relatively big constant. It can be substituted by the upper bound of the left-hand side of the inequality. Then we get  $Cons^S$ .

After solving the **MPs**, derive an optimal solution  $(l^*, s^*)$  and update  $UB_s = \sigma^*$ . If  $UB_s - LB_s \leq \epsilon_s$ , return and terminate.

- 3) *Step 3*: Obtain  $(\hat{l}, \hat{s})$  from *Step 2* and solve the subproblem of **SP**:

$$\textbf{SPs:} \quad \min_{(Z, P) \in F(\hat{x}, \hat{l}, \hat{s})} m \sum_t [P_{0,t,r}^{SUB} r_t^e + (\sum_i P_{0,i,t,r}^{CCHP} + \sum_j P_{0,j,t,r}^{GB}) r_t^g + P_{1,t,r}^{LS,d} p_t^{LS,d}], \quad (20a)$$

$$s.t. \quad \hat{\mathbf{L}} \leq \mathbf{C}^{SUB} \mathbf{P}_{0,r}^{SUB} + \mathbf{C} \mathbf{P}_{0,r}^{Equi} - \mathbf{P}_{0,r}^{ESS}, \quad (20b)$$

$$\hat{\mathbf{L}} \leq \mathbf{C}^{SUB} \mathbf{P}_{1,r}^{SUB} + \mathbf{C} \mathbf{P}_{1,r}^{Equi} - \mathbf{P}_{1,r}^{ESS} + \mathbf{P}_{1,r}^{LS}, \quad (20c)$$

$$P_{n,min}^{Equi} \hat{X}_n^{Equi} \leq P_{0,n,t,r}^{Equi} \leq P_{n,max}^{Equi} \hat{X}_n^{Equi}, \quad (20d)$$

$$P_{n,min}^{Equi} \hat{s}_{n,t}^{Equi} \hat{X}_n^{Equi} \leq P_{1,n,t,r}^{Equi} \leq P_{n,max}^{Equi} \hat{s}_{n,t}^{Equi} \hat{X}_n^{Equi}, \quad (20e)$$

$$Cons_{0,r}^{ESS}(\hat{X}^{B/T}, P_{0,ch/dis,t,r}^{B/T}, Z_{0,ch,t,r}^{B/T}, E_{0,t,r}^{B/T}), \quad (20f)$$

$$Cons_{1,r}^{ESS}(\hat{X}^{B/T}, P_{1,ch/dis,t,r}^{B/T}, Z_{1,ch,t,r}^{B/T}, E_{1,t,r}^{B/T}), \quad (20g)$$

$$0 \leq P_{0/1,t,r}^{SUB} \quad (20h)$$

$$0 \leq P_{1,t,r}^{LS,d} \quad (20i)$$

$$Z_{0/1,ch,t,q}^{B/T} \in \{0, 1\}. \quad (20j)$$

The **SPs** tends to optimize the second-stage variable  $Z$  based on given  $\hat{\mathbf{L}}$ ,  $\hat{s}^{Equi}$  from **MPs** and  $\hat{X}^{Equi}$  from **MP**. After solving **SPs**, derive an optimal solution  $(Z^*, P^*)$  and update  $LB_s = \max\{LB_s, m \sum_t [P_{0,t,r}^{SUB,*} r_t^e + (\sum_i P_{0,i,t,r}^{CCHP,*} + \sum_j P_{0,j,t,r}^{GB,*}) r_t^g] + P_{1,t,r}^{LS,d,*} p_t^{LS,d}\}$ . If  $UB_s - LB_s \leq \epsilon_s$ , return and terminate.

- 4) *Step 4*: Obtain  $\tilde{Z}$  from **SPs**, update  $p_s = p_s + 1$ . Create variables  $P^{r+1}$  and add constraints (14b)–(14l) with index  $r = r + 1$  to the **MPs**, go to *Step 2*.

Please refer to Algorithm 2 for a more concise solution process.

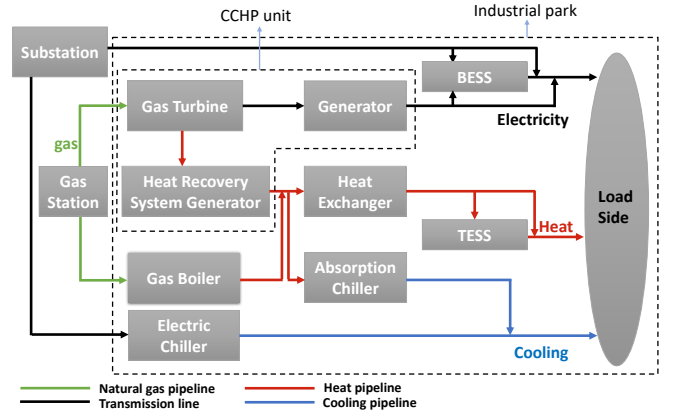


Fig. 1. Schematic of a industrial park.

#### Algorithm 2 Inner layer C&CG

**Input:**  $LB_s = -\inf, UB_s = +\inf, \epsilon_s = 0.0001, p_s = 0$

**Output:**  $l^*, s^*$

- 1: **while**  $UB_s - LB_s \leq \epsilon_s$  **do**
- 2: Solve the **MPs** with  $\tilde{Z}$
- 3: Update  $UB_s \rightarrow \theta^*$
- 4: Solve the **SPs** with  $(\hat{X}, \hat{l}, \hat{s})$
- 5: Update  $LB_s \rightarrow \max\{LB_s, \sigma^*\}$
- 6: Create variables  $P^{r+1}$  and add constraints back to **MPs**
- 7: Update  $p_s \rightarrow p_s + 1$
- 8: **end while**

## IV. CASE STUDY

### A. Case Condition

An industrial park from our previous work [12] is used as the numerical case. Substation and natural gas station outside the park provide electricity and natural gas respectively as input for the park. Electricity, heat, and cooling energy are needed on the demand side. Four representative days with various load demand data are given as a baseline. The maximum electric, heat, and cooling loads of the park are 60MW, 85MW, and 75MW respectively. The equipment to be selected in the park includes CCHP units, gas boilers, and electric chillers, of which there are 7 types of CCHP units, 10 types of gas boilers and electric chillers. The parameters of equipment can be found in relevant study [27]. The specific equipment connection of the park is shown in Fig. 1.

To formulate proper equipment contingency uncertainty set for the proposed two-stage robust planning model, we refer to relevant parameters in another study [28], i.e. the failure and repair rates of different equipment. We set  $\Gamma^N$  as 1, which means we mainly focus on the operation scenarios with at most one contingency in the same period. Besides, we note that considering load fluctuation uncertainty in our case will make the model too conservative. Since the multi-energy load uncertainty set is not the highlight of this study, we will not consider it in this case, i.e., set  $\Gamma^l$  as 0. For other parameters, there is no standard approach to convert these annualized reliability parameters to the parameters of representative days. Consequently, we adjust these uncertainty budgets to assess their impact on planning results, which will be further discussed in the subsequent section.

TABLE I  
THE PLANNING RESULTS FOR CCHP UNITS.

Capacity	5	10	15	20	25	30	35	Total/MW
Case 1-4	0	0	1	0	0	0	1	50

TABLE II  
THE PLANNING RESULTS FOR GAS BOILERS.

Capacity	10	20	30	40	50	60	70	80-100	Total/MW
Case 1	0	0	0	0	1	0	0	0	50
Case 2	1	0	1	0	0	0	0	0	40
Case 3	1	1	1	0	0	0	0	0	60
Case 4	1	1	1	0	0	0	0	0	60

### B. Analysis on Planning Results

After the experiment, we observed that the duration of equipment contingency,  $\Gamma_n^D$ , significantly affects the final planning scheme, whereas the interval between two equipment contingencies,  $\Gamma_n^I$ , has no impact on the result. This suggests that prolonged equipment contingencies necessitate capacity expansion to provide more reserve, while a short interval between sequential contingencies does not affect energy supply as long as total capacity remains sufficient. Therefore, we observe planning schemes variations for different  $\Gamma_n^D$  values in the following cases:

- 1) *Case 1*: Deterministic planning model, i.e.,  $\Gamma_n^D = 0$ ;
- 2) *Case 2*: Two-stage robust planning model with uncertainty budget:  $\{\Gamma_n^D \leq 2\}$ ;
- 3) *Case 3*: Two-stage robust planning model with uncertainty budget:  $\{\Gamma_n^D = 4\}$ ;
- 4) *Case 4*: Two-stage robust planning model with uncertainty budget:  $\{\Gamma_n^D \geq 6\}$ ;

The planning results are shown in Table I-IV. In these tables, ‘1’ indicates equipment construction, while ‘0’ indicates no construction. As for CCHP units, different models make the same decision. This is because the investment cost of CCHP unit is high and thus the planning scheme cannot be easily altered. Besides, the planning scheme with two CCHP units is relatively reliable.

Regarding gas boilers, only one single gas boiler of 50 MW capacity is constructed under the deterministic planning scheme. In contrast, the robust planning schemes replace the large capacity gas boiler with several gas boilers in relatively small capacity to mitigate potential shedding load caused by single equipment contingency. This necessitates an expansion of the total capacity of GB or TESS to improve IES reliability. To be more specific, when relatively short failure is considered, *Case 2* chooses to replace the 50MW boiler with two boilers of 10MW and 30MW. The total capacity of GB decreases and larger TESS is invested. The role of TESS will be analyzed in the next part. When considering contingency for more than 4 hours, merely replacing the larger boiler with smaller ones is insufficient. So, *Case 3 and 4* both choose to invest in three boilers of 10MW, 20MW, and 30MW in order to avoid the huge potential load shedding caused by the failure of each single unit. They also choose to enlarge the capacity of TESS compared with *Case 1*.

The planning schemes of electric chillers show exactly the same trend as those of gas boilers. When uncertain equipment contingency is considered, the total capacity of EC should be increased to 60MW to ensure the normal cooling energy supply. As for the planning schemes of ESS, more than 8 MW BESS should be invested to earn profit from the time-of-use electricity tariff. The capacity of invested TESS is affected by the uncertainty budget  $\Gamma_n^D$ , i.e., the duration of equipment contingency. We will analyze it later.

The total cost of different planning schemes can be shown in Table V. Obviously, the planning schemes from robust models increase the investment cost to improve reliability. It should also be noted that even the most robust planning scheme, *Case 4*, only increases the total cost by less than 1% compared to the deterministic scheme. To better compare these planning schemes, we will evaluate their reliability in the next part.

### C. Reliability Assessment

The MCS method which is simple and efficient is applied to quantify the reliability level of the planning schemes obtained above. The reliability indices we use include EENS, LOLE, and LOLE, which can well reflect the total amount, frequency and duration of different types of energy load shedding. The essence of the MCS is to simulate the actual operation situation with a large number of scenarios. The obtained planning results will be run under all generated operation scenarios and the values of the reliability indices will be calculated. When the sample size is large enough, the obtained results of the reliability level converge to the true values.

The generated operation scenarios should include electricity, heat, and cooling load demand at any time  $t$ . Besides, it is also necessary for these scenarios to include the operating states of equipment that have been invested. In this case study, we assume that all three loads follow a normal distribution with fluctuations within  $\pm 5\%$ ,  $\pm 8\%$ , and  $\pm 5\%$  respectively. To simulate the operating states of each invested equipment, we use the widely used two-status model, where equipment transitions between “normal” and “fault” states, with transformation probabilities governed by parameters such as equipment failure rates and repair rates. Detailed methods and relevant parameters can be found in [18] and [28] respectively.

We choose the sample size as 500 years (each year with 8760 hours) to calculate these reliability indices. The evaluation results of obtained planning schemes are shown in Table VI.

Because this IES is not operated in an isolated mode, the substation outside the IES can supply the electricity demand. So, there will be no electricity load shedding in this case and we will focus on the reliability of the supply of thermal load and cooling load. It can be seen that there will be severe thermal load shedding as well as cooling load shedding in *Case 1*. There is also a high frequency of load shedding occurrence within a year. This is unacceptable for most IES, especially for IES with high-reliability requirements, where a small amount of load shedding can result in significant economic losses. The reason for this result is that this case does not consider possible equipment contingencies and load fluctuations. Therefore leads to an unreliable planning scheme.



TABLE III  
THE PLANNING RESULTS FOR ELECTRIC CHILLERS.

Capacity	2.5	5.0	7.5	10.0	12.5	15.0	17.5	20.0	22.5	25.0	Total/MW
Case 1	0	0	0	0	0	0	0	0	1	0	22.5
Case 2	0	0	1	0	1	1	0	0	0	1	60
Case 3	1	1	1	0	0	0	0	1	0	1	60
Case 4	1	0	0	1	0	0	0	0	1	1	60

TABLE IV  
THE PLANNING RESULTS FOR ESS.

	Case 1	Case 2	Case 3	Case 4
BESS/MWh	8.62	8.62	8.62	8.62
TESS/MWh	3.05	69.81	33.00	36.01

TABLE V  
COST OF DIFFERENT PLANNING SCHEMES (UNIT:  $\text{¥}10^4$ ).

	Investment		Operational cost	Total	
	Cost	Increment		Cost	Increment
Case 1	58482.4	-	183504.6	241887.0	-
Case 2	62265.3	6.47%	181651.5	243916.8	0.84%
Case 3	61593.2	5.32%	182655.5	244248.7	0.98%
Case 4	61715.9	5.53%	182572.2	244287.1	0.99%

By considering potential uncertainties, *Case 1-3* significantly reduce all three relevant indices of both heat and cooling load. For *Case 2*, it enlarges the capacity of TESS and reduces the heat EENS, LOLE, and LOLF by 92.4%, 93.5% and 93.1% respectively. *Case 3 and 4* reduce the shedding load of both the heat and cooling to almost zero. From the last part, these two cases improve the system reliability by only increasing around 1% total cost.

#### D. Analysis on TESS

The capacity of TESS and the selection of GB invested under different uncertainty budgets are given in Table VII. In the deterministic model, i.e.,  $\Gamma_n^D = 0$ , 3.05MW TESS is invested. It can be used to save operational costs by storing heat surplus from CCHP and releasing it when heat is needed. This is the first function of TESS, and also the most commonly discussed one. When relatively short equipment contingency, which is not longer than 3 hours, is considered, large capacity TESS will be invested. On the one hand, large capacity TESS is used to provide reserve to against short-term failures of other equipment. On the other hand, it can fill the heat supply

TABLE VI  
THE RESULTS OF RELIABILITY EVALUATION

		EENS (MW/year)	LOLE (hours/year)	LOLF (occ/year)
Heat	Case 1	62.58	5.97	2.75
	2	4.74	0.39	0.19
	3	0.20	0.04	0.03
	4	0.06	0.03	0.01
Cooling	1	19.71	3.71	2.35
	2	0.03	0.01	0.01
	3	0.03	0.01	0.01
	4	0.03	0.01	0.01

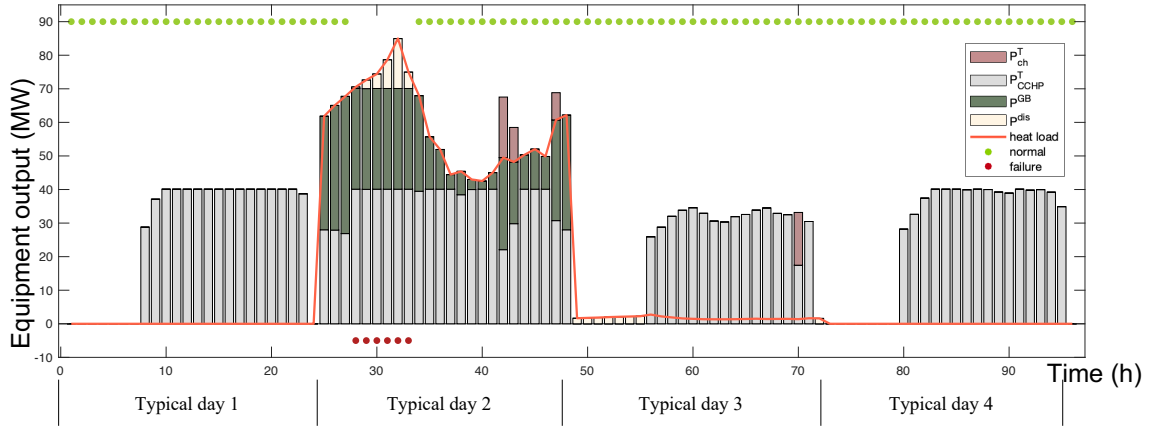
TABLE VII  
THE CAPACITY OF TESS AND GB UNDER DIFFERENT  $\Gamma_n^D$ .

$\Gamma_n^D$	TESS/MWh	GB/MW
0	3.05	50
1,2	69.81	10+30
3	89.24	10+30
4	33.00	10+20+30
5	35.58	10+20+30
6	36.01	10+20+30

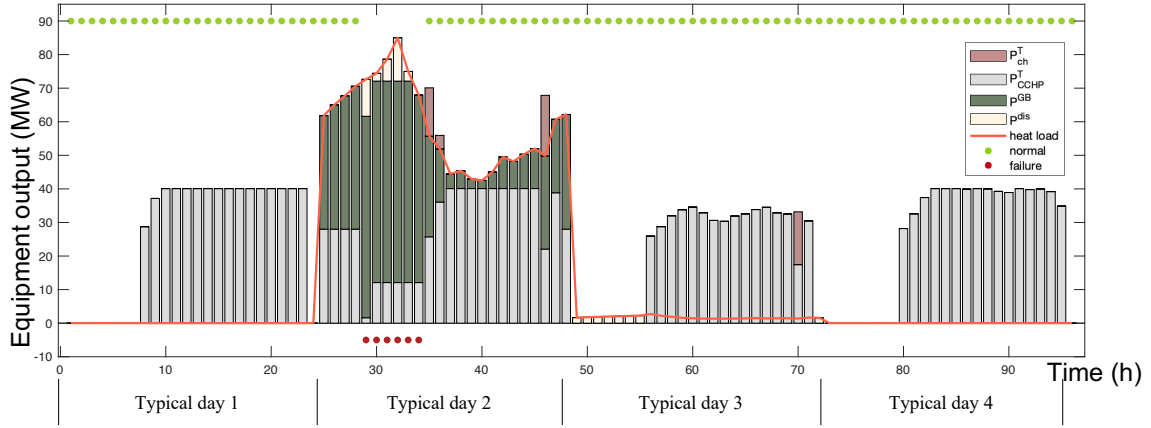
gap caused by the reduction in total GB capacity compared to the deterministic planning scheme. When longer periods of contingency are considered, raising the capacity of TESS alone cannot avoid potential load shedding, so the capacity of the GB is increased accordingly. By comparing the two cases of  $\Gamma_n^D = 2$  and  $\Gamma_n^D = 3$ , it is obvious that in the case of the same GB capacity invested, the longer the contingency period is considered, the larger the capacity of the TESS should be built. The same conclusion can also be obtained by comparing the three cases of  $\Gamma_n^D = 4$ ,  $\Gamma_n^D = 5$ , and  $\Gamma_n^D = 6$ . It leads to the second function of TESS, improving IES reliability by providing reserve.

We choose the case with  $\Gamma_n^D = 6$  to further analyze this function of TESS. Fig. 2 shows the optimal operation scheme under this planning scheme when the worst-case equipment contingency is considered. Fig. 2(a) shows the operation scenario that includes the contingency of the third GB, whose capacity is 30MW. The worst case is found by the solution process of the planning problem. It can be seen that under the worst case, the 30MW GB is out of operation while the heat load peaks. In this situation, the normally operating boilers and CCHP units are only capable of providing 70 MW of heat power, which is below the peak hour demand. Now, the heat previously stored in TESS comes into play. The heat release from the TESS, which is represented by the beige bars, fills the gap of the heat supply, thus ensuring that the system can supply the energy demand normally when equipment contingency happens.

Fig. 2(b) shows the operation scenario that includes the contingency of the 35MW CCHP unit. The contingency happens at almost the same time as the GB contingency that we discussed above to cause a maximum shortage of heat supply. During this CCHP contingency, all the remaining normal equipment can only supply about 70MW of heat power, and the remaining gap is also filled by the heat reserve in advance. In this case, the function of TESS in terms of improving reliability and saving total cost is verified.



(a) The operation scheme in case of contingency of the third GB (30MW)



(b) The operation scheme in case of contingency of the second CCHP unit (35MW)

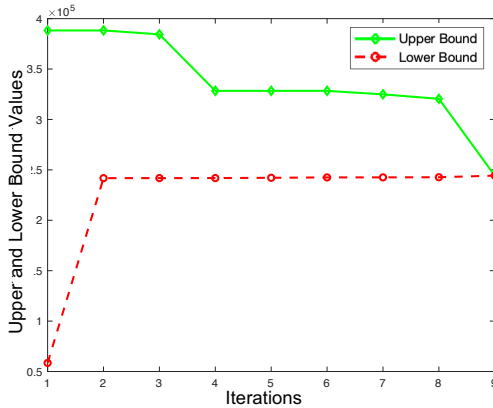
Fig. 2. The optimal operation scheme under the planning scheme of  $\Gamma_n^D = 6$  when the worst-case equipment contingency is considered.

Fig. 3. Convergence process of the outer layer algorithm.

### E. Convergence Performance of Nested C&CG

We choose the case with  $\Gamma_n^D = 6$  to assess the performance of the nested C&CG approach in solving the proposed two-stage robust IES planning model in this part. Regarding convergence performance, the outer layer algorithm requires a total of 8 iterations before reaching convergence. The upper and lower bound values are depicted in Fig. 3.

The master problem used to optimize the first stage decision variables yields a lower bound. This lower bound gradually increases as the planning scheme becomes more reliable. Conversely, the subproblem boosts the total cost by finding the worst operation scenario with equipment contingency. In this process, the load shedding occurs and costs a high penalty and therefore gets an upper bound with a large value. As the planning scheme gradually becomes reliable, there will be no load shedding even in the worst operation scenario and the problem converges to the optimum.

Based on the principle of the nested C&CG algorithm, each outer iteration involves multiple iterations of the inner C&CG algorithm, which are used to solve the subproblem. In our case, all inner subproblems are solved after only 2-3 iterations. The convergence of the inner layer algorithm is very fast, and the gap becomes relatively small after only 1-2 iterations.

In this case, the master problem is less time-consuming compared to the subproblem. This is because the subproblem is reformulated into a tri-level problem, and its solution process is another C&CG. As we mentioned, both KKT conditions and strong duality property can be applied to reformulate the subproblem. Based on these two methods, the computational time of the subproblem in each outer iteration is shown in Fig. 4. It is obvious that the solution speed

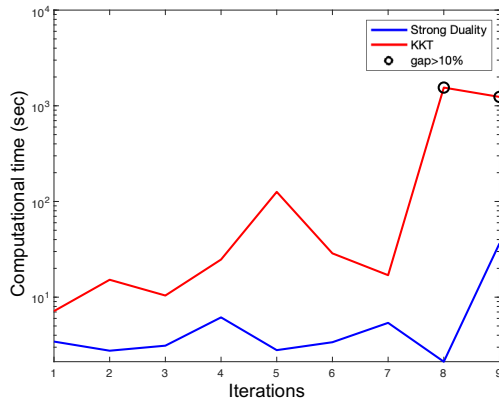


Fig. 4. Computational time of subproblem reformulated by different methods in each outer layer iteration.

of the strong duality-based subproblem is much faster than that of KKT-based subproblem. Moreover, the KKT-based subproblem still maintains a gap of over 10% after more than 1000 seconds of computation in the last two iterations. Other iterations that are not circled eventually converge to a gap of 0.01%.

Both subproblem reformulation based on KKT conditions and strong duality property introduce bilinear terms into the planning model. The big-M method which will introduce binary variables and increase the problem complexity is used to eliminate these terms. Therefore, the difference in computational time mainly comes from the number of binary variables introduced by these two reformulation methods. In this case, the continuous variables introduced by these two reformulation methods are almost the same. However, KKT introduces over 14000 binary variables, whereas that strong duality introduces less than 3000 binary variables in each inner layer iteration, which is a huge difference. While the magnitude of this difference may vary from case to case, reference [29] confirms that the strong duality-based reformulation outperforms the KKT-based reformulation in terms of the number of introduced binary variables.

## V. CONCLUSION

Reliability is one of the most important performance indicators for IES, as it directly affects energy supply and is closely related to the functioning of society and people's lives. This paper proposes a two-stage robust planning model for park-level IES, which can avoid the failure of the system under the interference of uncertainty such as equipment contingency. The conclusions drawn from the numerical case are threefold:

- 1) The proposed two-stage robust IES planning model outperforms the deterministic counterpart in improving system reliability. In particular, the robust planning scheme that considers short-term equipment contingency significantly reduces three metrics, EENS, LOLE, and LOLF, by over 90% compared to the deterministic planning scheme, with a marginal increase in total cost of only 0.84%. The most robust scheme nearly eliminates these metrics and increases the total cost by less than 1%;

- 2) The ESS plays an important role in IES. In this study, TESS is used as an example to analyze its role in saving operating costs and improving reliability;
- 3) The nested C&CG algorithm shows good performance in solving two-stage robust IES planning problem with second stage integer variables. In the case study, the solution times of subproblems reformulated by different approaches: KKT conditions and strong duality, are compared. It helps us to further corroborate the superiority of the C&CG algorithm whose subproblem is reformulated by strong duality.

Future work would further explore the generality and scalability of the proposed robust planning model. The proposed model will be applied to more complex and larger energy systems, and the proposed uncertainty set will be used to describe all kinds of possible contingencies, e.g., transmission line outage. As the size of the problem increases, the corresponding algorithm should also be further developed to improve the solving speed.

## ACKNOWLEDGMENT

The authors would like to acknowledge the help of Prof. Line Roald, both in discussions leading to the development of the paper as well as feedback on the paper draft.

## REFERENCES

- [1] H. Sun, Q. Guo, and Z. Pan, "Energy internet: concept, architecture and frontier outlook," *Automation of Electric Power Systems*, 2015.
- [2] L. A. Roald, D. Pozo, A. Papavasiliou, D. K. Molzahn, J. Kazempour, and A. Conejo, "Power systems optimization under uncertainty: A review of methods and applications," *Electric Power Systems Research*, vol. 214, p. 108725, 2023. [Online]. Available: <https://www.sciencedirect.com/science/article/pii/S0378779622007842>
- [3] S. Yang, Z. Tan, H. Lin, P. Li, G. De, F. Zhou, and L. Ju, "A two-stage optimization model for park integrated energy system operation and benefit allocation considering the effect of time-of-use energy price," *Energy*, vol. 195, p. 117013, 2020. [Online]. Available: <https://www.sciencedirect.com/science/article/pii/S0360544220301201>
- [4] W. Li, *Reliability assessment of electric power systems using Monte Carlo methods*. Springer Science & Business Media, 2013.
- [5] Y. Chen, Y. Zheng, F. Luo, J. Wen, and Z. Xu, "Reliability evaluation of distribution systems with mobile energy storage systems," *IET Renewable Power Generation*, vol. 10, no. 10, pp. 1562–1569, 2016.
- [6] G. Sansavini, R. Piccinelli, L. R. Golea, and E. Zio, "A stochastic framework for uncertainty analysis in electric power transmission systems with wind generation," *Renewable Energy*, vol. 64, pp. 71–81, 2014. [Online]. Available: <https://www.sciencedirect.com/science/article/pii/S0960148113005806>
- [7] G. Koeppl and G. Andersson, "Reliability modeling of multi-carrier energy systems," *Energy*, vol. 34, no. 3, pp. 235–244, 2009. [Online]. Available: <https://www.sciencedirect.com/science/article/pii/S0360544208001151>
- [8] R. A. Jabr, I. Džafić, and B. C. Pal, "Robust optimization of storage investment on transmission networks," *IEEE Transactions on Power Systems*, vol. 30, no. 1, pp. 531–539, 2015.
- [9] S. Moret, F. Babonneau, M. Bierlaire, and F. Maréchal, "Decision support for strategic energy planning: A robust optimization framework," *European Journal of Operational Research*, vol. 280, no. 2, pp. 539–554, 2020. [Online]. Available: <https://www.sciencedirect.com/science/article/pii/S0377221719304904>
- [10] —, "Overcapacity in european power systems: Analysis and robust optimization approach," *Applied Energy*, vol. 259, p. 113970, 2020. [Online]. Available: <https://www.sciencedirect.com/science/article/pii/S0360261919316575>
- [11] Y. Zhang, Y. Hu, J. Ma, and Z. Bie, "A mixed-integer linear programming approach to security-constrained co-optimization expansion planning of natural gas and electricity transmission systems," *IEEE Transactions on Power Systems*, vol. 33, no. 6, pp. 6368–6378, 2018.

- [12] Z. Xiong, X. Shen, B. Wang, Q. Guo, H. Sun, and Z. Pan, "Optimal planning of electric-heat coupled integrated energy system with n-1 constraints," in *2020 IEEE 4th Conference on Energy Internet and Energy System Integration (EI2)*, 2020, Conference Proceedings, pp. 221–226.
- [13] R. L. Chen, A. Cohn, N. Fan, and A. Pinar, "Contingency-risk informed power system design," *IEEE Transactions on Power Systems*, vol. 29, no. 5, pp. 2087–2096, 2014.
- [14] S. Bahramirad, W. Reder, and A. Khodaei, "Reliability-constrained optimal sizing of energy storage system in a microgrid," *IEEE Transactions on Smart Grid*, vol. 3, no. 4, pp. 2056–2062, 2012.
- [15] S. Dehghan, N. Amjadi, and A. J. Conejo, "Reliability-constrained robust power system expansion planning," *IEEE Transactions on Power Systems*, vol. 31, no. 3, pp. 2383–2392, 2016.
- [16] C. He, L. Wu, T. Liu, and Z. Bie, "Robust co-optimization planning of interdependent electricity and natural gas systems with a joint n-1 and probabilistic reliability criterion," *IEEE Transactions on Power Systems*, vol. 33, no. 2, pp. 2140–2154, 2018.
- [17] L. C. d. Costa, F. S. Thomé, J. D. Garcia, and M. V. F. Pereira, "Reliability-constrained power system expansion planning: A stochastic risk-averse optimization approach," *IEEE Transactions on Power Systems*, vol. 36, no. 1, pp. 97–106, 2021.
- [18] B. Yin, Y. Li, S. Miao, Y. Lin, and H. Zhao, "An economy and reliability co-optimization planning method of adiabatic compressed air energy storage for urban integrated energy system," *Journal of Energy Storage*, vol. 40, 2021.
- [19] X. Zhang, L. Che, M. Shahidehpour, A. S. Alabdulwahab, and A. Abu-sorrah, "Reliability-based optimal planning of electricity and natural gas interconnections for multiple energy hubs," *IEEE Transactions on Smart Grid*, vol. 8, no. 4, pp. 1658–1667, 2017.
- [20] M. Jooshaki, A. Abbaspour, M. Fotuhi-Firuzabad, G. Muñoz-Delgado, J. Contreras, M. Lehtonen, and J. M. Arroyo, "An enhanced milp model for multistage reliability-constrained distribution network expansion planning," *IEEE Transactions on Power Systems*, vol. 37, no. 1, pp. 118–131, 2022.
- [21] Z. Xiong, X. Shen, Q. Wu, Q. Guo, and H. Sun, "Stochastic planning for low-carbon building integrated energy system considering electric-heat-v2g coupling," *International Journal of Electrical Power & Energy Systems*, vol. 151, p. 109148, 2023. [Online]. Available: <https://www.sciencedirect.com/science/article/pii/S0142061523002053>
- [22] Y. Fang and G. Sansavini, "Optimizing power system investments and resilience against attacks," *Reliability Engineering & System Safety*, vol. 159, pp. 161–173, 2017. [Online]. Available: <https://www.sciencedirect.com/science/article/pii/S0951832016307244>
- [23] P. Favre-Perrod, "A vision of future energy networks," in *2005 IEEE Power Engineering Society Inaugural Conference and Exposition in Africa*, 2007, Conference Proceedings, pp. 13–17.
- [24] D. Bertsimas, E. Litvinov, X. A. Sun, J. Zhao, and T. Zheng, "Adaptive robust optimization for the security constrained unit commitment problem," *IEEE Transactions on Power Systems*, vol. 28, no. 1, pp. 52–63, 2013.
- [25] B. Zeng and L. Zhao, "Solving two-stage robust optimization problems using a column-and-constraint generation method," *Operations Research Letters*, vol. 41, no. 5, pp. 457–461, 2013. [Online]. Available: <https://www.sciencedirect.com/science/article/pii/S0167637713000618>
- [26] L. Zhao and B. Zeng, "An exact algorithm for two-stage robust optimization with mixed integer recourse problems," *submitted, available on Optimization-Online.org*, 2012.
- [27] X. Shen, Q. Guo, X. U. Yinliang, H. Sun, and T. University, "Robust planning method for regional integrated energy system considering multi-energy load uncertainties," *Automation of Electric Power Systems*, 2019.
- [28] J.-J. Wang, C. Fu, K. Yang, X.-T. Zhang, G.-h. Shi, and J. Zhai, "Reliability and availability analysis of redundant bchp (building cooling, heating and power) system," *Energy*, vol. 61, pp. 531–540, 2013. [Online]. Available: <https://www.sciencedirect.com/science/article/pii/S036054421300769X>
- [29] G. Huang, J. Wang, C. Chen, J. Qi, and C. Guo, "Integration of preventive and emergency responses for power grid resilience enhancement," *IEEE Transactions on Power Systems*, vol. 32, no. 6, pp. 4451–4463, 2017.

Department of Electrical Engineering, Tsinghua University, Beijing, China, in 2020, and the M.S. degree from Tsinghua-Berkeley Shenzhen Institute, Shenzhen International Graduate School, Tsinghua University, Shenzhen, China, in 2023. He is currently pursuing his Ph.D. in the Department of Engineering Science, University of Oxford. His research interests include optimization in power system and data-driven control theory. He was the recipient of the Best Paper Award at the 4th IEEE EI2 Conference.

**Xinwei Shen** (Senior Member, IEEE) received the B.E. and Ph.D. degrees from the Department of Electrical Engineering, Tsinghua University, Beijing, China, in 2010 and 2016, respectively. He was a Visiting Scholar with the IIT, University of California, Berkeley, Berkeley, CA, USA, and University of Macau, Macau, China, in 2014, 2017, and 2021, respectively. He is currently an Assistant Professor with Tsinghua Shenzhen International Graduate School, Tsinghua University. His research interests include energy internet, integrated energy system/power distribution system optimization with energy storage and renewables. In 2020, he was awarded the Young Elite Scientists Sponsorship Program by Chinese Society for Electrical Engineering (CSEE). He is currently the Co-Chair of IEEE PES Working Group on Integrated Energy System/Multi-Energy Network Modeling and Planning and officer of PES Energy Internet Coordinating Committee (EICC). He is the Subject Editor of the *CSEE Journal of Power and Energy Systems* and Young Editorial Board Member of *Applied Energy*.

**Hongbin Sun** (Fellow, IEEE) received the double B.S. degrees from Tsinghua University, Beijing, China, in 1992, and the Ph.D. degree from the Department of Electrical Engineering, Tsinghua University in 1997, where he is currently a Changjiang Scholar Chair Professor with the Education Ministry of China, a tenured Full Professor of Electrical Engineering, and the Director of Energy Management and Control Research Center. He is also with the College of Electrical Engineering, Taiyuan University of Technology. From 2007 to 2008, he was a Visiting Professor with the School of Electrical Engineering and Computer Science, Washington State University, Pullman, WA, USA. Over the last 20 years, he led a research group with Tsinghua University to develop a commercial system-wide automatic voltage control system, which has been applied to more than 100 electrical power control centers in China and the control center of PJM interconnection, the largest regional power grid in the U.S. He has authored or coauthored more than 300 peer-reviewed papers. His research interests include energy management system, automatic voltage control, energy Internet, and energy system integration. He won the China National Technology Innovation Award in 2008, the National Distinguished Teacher Award of China in 2009, and the National Science Fund for Distinguished Young Scholars of China in 2010. He is the Chair of the IEEE Smart Grid Voltage Control Task Force and IEEE Energy Internet Working Group. In November 2017, he was the Founding Chair of the IEEE Conference on Energy Internet and Energy System Integration. He is also a Fellow of IET.